UTILITY OF TSAI'S METHOD FOR SEISMIC DISCRIMINATION

Semi-Annual Technical Report No. 1

1 July 1971 to 31 December 1971

Yi-Ben Tsai
Project Scientist
Area Code 703, 836-3882 Ext-305

T. W. Harley, Program Manager
Area Code 703, 836-3882 Ext-300

TEXAS INSTRUMENTS INCORPORATED
Services Group
P. O. Box 5621
Dallas, Texas 75222

Contract No. F44620-71-C-0112
Amount of Contract: $47,967
Beginning 1 July 1971
Ending 30 June 1972

Prepared for

AIR FORCE OFFICE OF SCIENTIFIC RESEARCH

Sponsored by

ADVANCED RESEARCH PROJECTS AGENCY
Nuclear Monitoring Research Office
ARPA Order No. 1827
ARPA Program Code No. 1F10

15 January 1972

Acknowledgement: This research was supported by the Advanced Research Projects Agency, Nuclear Monitoring Research Office, under Project VELA-UNIFORM, and accomplished under the direction of the Air Force Office of Scientific Research under Contract No. F44620-71-C-0112.

UTILITY OF TSAI'S METHOD FOR SEISMIC DISCRIMINATION

Semi-Annual Technical Report No. 1

1 July 1971 to 31 December 1971

Yi-Ben Tsai
Project Scientist
Area Code 703, 836-3882 Ext-305

T. W. Harley, Program Manager
Area Code 703, 836-3882 Ext-300

TEXAS INSTRUMENTS INCORPORATED
Services Group
P.O. Box 5621
Dallas, Texas 75222

Contract No. F44620-71-C-0112
Amount of Contract: $47,967
Beginning 1 July 1971
Ending 30 June 1972

Prepared for

AIR FORCE OFFICE OF SCIENTIFIC RESEARCH

Sponsored by

ADVANCED RESEARCH PROJECTS AGENCY
Nuclear Monitoring Research Office
ARPA Order No. 1827
ARPA Program Code No. 1F10

15 January 1972

Acknowledgement: This research was supported by the Advanced Research Projects Agency, Nuclear Monitoring Research Office, under Project VELA-UNIFORM, and accomplished under the direction of the Air Force Office of Scientific Research under Contract No. F44620-71-C-0112.

UNCLASSIFIED
Security Classification

DOCUMENT CONTROL DATA – R & D
(Security classification of title, body of abstract and indexing annotation must be entered when the overall report is classified)

1. ORIGINATING ACTIVITY (Corporate author)
Texas Instruments Incorporated
Services Group
P.O. Box 5621, Dallas, Texas 75222

2a. REPORT SECURITY CLASSIFICATION
UNCLASSIFIED

2b. GROUP

3. REPORT TITLE
Utility of Tsai's method for Seismic Discrimination
Semi-Annual Technical Report No. 1

4. DESCRIPTIVE NOTES (Type of report and inclusive dates)
Semi-Annual Technical Report No. 1, 1 July 1971 through 31 December 1971

5. AUTHOR(S) (First name, middle initial, last name)
Tsai, Yi-Ben

6. REPORT DATE
31 January 1972

7a. TOTAL NO. OF PAGES
37

7b. NO. OF REFS
8

8a. CONTRACT OR GRANT NO.
F44620-71-C-0112

b. PROJECT NO.

c.

d.

9a. ORIGINATOR'S REPORT NUMBER(S)

9b. OTHER REPORT NO(S) (Any other numbers that may be assigned this report)

10. DISTRIBUTION STATEMENT
Approved for public release ; distribution unlimited

11. SUPPLEMENTARY NOTES
ARPA order No. 1827

12. SPONSORING MILITARY ACTIVITY
Advanced Research Projects Agency
AFOSR Contract F44620-71-C-0112

13. ABSTRACT

This semi-annual report summarizes technical progress made during the period 1 July 1971 to 31 December 1971 on Contract F44620-71-C-0112.

DD FORM 1 NOV 65 1473

UNCLASSIFIED
Security Classification

14. KEY WORDS	LINK A		LINK B		LINK C	
	ROLE	WT	ROLE	WT	ROLE	WT
• Rayleigh wave spectra						
• Love wave spectra						
• Complex cepstrum technique						
• Regionalization of Earthquake Surface wave spectra						
• Discrimination using Rayleigh and Love wave spectra						

CONTENTS

LIST OF FIGURES

LIST OF TABLES

I. INTRODUCTION AND SUMMARY

The objective of the program is to study how the surface wave spectral analysis technique can be most effectively exploited to discriminate between earthquakes and underground nuclear explosions.

The observed surface wave spectra are often contaminated by modulations caused by interference due to multipath propagation. These spectral modulations are not related to the characteristics of the seismic source, which is our prime concern, and so, our first task is to find an effective means for removing the undesirable modulations of the spectra. It has been found that the complex cepstrum technique suits our purpose well. The technique was developed by Schafer (1969) and shown to be very effective in removing multipath Rayleigh waves by Linville (1971). Section II describes the technique briefly, and presents two examples of actual surface waveforms to illustrate the effects of interference on spectra and the effectiveness of the complex cepstrum technique in removing these effects.

The crust-upper mantle structure as well as the source mechanism of earthquakes vary significantly from region to region. Moreover, we are most interested in seismic events of medium to low magnitudes. For these relatively small events surface-wave data of satisfactory quality are expected to be available only from recording sites located not too far from the epicenter. It becomes evident from the preceding considerations that discrimination between earthquakes and underground nuclear explosions using the surface wave spectral analysis technique can be accomplished most effectively on a regional basis. Thus we have set out to establish an ensemble of surface wave spectral data from earthquakes in the Arctic Ocean and in the Eurasian Continent stretching from Turkey in the west to Southwestern China in the east. In total, Rayleigh and Love wave spectra of twenty-eight seismic events have been studied; the details of this analysis are given in Section III.

Our goal is to extract information about the source mechanism and focal depth of a seismic event from surface wave spectra observed at a limited number of recording sites. In addition to serving as an independent discriminant, this information may help interpret other observed seismic data and so improve the outcome of seismic discrimination. An automatic searching scheme has been devised to achieve this goal. Tests of the scheme have also been carried out on a number of earthquakes. Section IV describes this automatic searching scheme and the testing results yielded by its application.

Major conclusions from the study conducted in the past six months are summarized in Section V. Future plans are also outlined in this section.

II. APPLICATION OF THE COMPLEX CEPSTRUM TECHNIQUE FOR THE SPECTRAL ANALYSIS OF SURFACE WAVES

Utility of amplitude spectra of surface waves to determine the seismic source parameters such as seismic moment, focal depth, etc. is often hindered by spectral modulations caused by interference of secondary wave trains due to either multiple events or multipath propagation of a single event or both. Such spectral modulations are not related to the characteristics of the source itself and therefore have to be removed before the spectra can be used for extracting information about the source. To overcome this difficulty it is found that the complex cepstrum technique is quite effective. In this section the results from application of the technique to actual surface waveforms are described.

The mathematical foundation of the complex cepstrum technique has been established by Schafer (1969). Linville (1971) and his colleagues at Texas Instruments, Incorporated have successfully applied the technique to study multipath Rayleigh waves. Since detailed discussions on both theoretical and practical aspects of the technique have been made by the authors referred to above, only a brief summary of the technique is given here:

- The modulated waveform x(t) is mathematically represented as the convolution of the primary waveform s(t) and a multipath operator m(t), i.e.

  $$x(t) = s(t) * m(t) \quad (1)$$

  In the frequency domain this equation becomes

  $$X(w) = S(w)\, M(w) \quad (2)$$

- The logarithm of X(w) is taken, thus

  $$\log X(w) = \log S(w) + \log M(w) \quad (3)$$

  The imaginary part of log X(w) is made continuous and its linear component is removed.

- The modified function of log X(w) is treated as a complex time series. Its inverse Fourier transform is taken to yield a function call the complex cepstrum.
- A linear filter then is applied to the complex cepstrum to separate log S(w) and log M(w). The separation can be achieved so long as these two components have sufficiently different spectral content.
- The exponential is taken to get back to an estimate of S(w) or M(w) which is subsequently transformed back into the time domain and thus yield the primary waveform s(t) or the multipath operator m(t).

The computer program written by Linville (1971) is adopted with minor modifications for our applications. The technique is applied whenever the surface wave trains appear to have been contaminated by interference of multiple arrivals.

Two examples are given here to illustrate the effectiveness of the complex cepstrum technique for separating multiple wavetrains. Figure 1 shows the results obtained from application of the technique to Rayleigh waves from two successive earthquakes at the same epicenter on the North Atlantic Ridge recorded at Ogdensburg (OGD). PDE gives the following source parameters for these events:

Event 1	70-12-22	20:51:16.2	28.3N	43.9W	5.3 (m_b)
Event 2	70-12-22	20:53:04.3	28.3N	43.9W	5.4 (m_b)

Trace A in Figure 1 shows the composite waveform of the two Rayleigh wavetrains. This waveform was obtained from the original digital record after filtering with a 0.02 to 0.05 Hz bandpass filter. Trace B is the primary waveform s(t) recovered by the complex cepstrum technique. Trace C is obtained by subtracting Trace B from Trace A. The resemblance between Trace B and Trace C is remarkable.

FIGURE 1

Results of application of the complex cepstrum technique. A. - Rayleigh waves from two earthquakes on the North-Atlantic ridge recorded at OGD. B. - Rayleigh waves of the second eartnquake recovered from Trace A by the complex cepstrum technique; C. - Difference between Trace A and Trace B; D. - Waveform of the multipath operator obtained by the complex cepstrum technique.

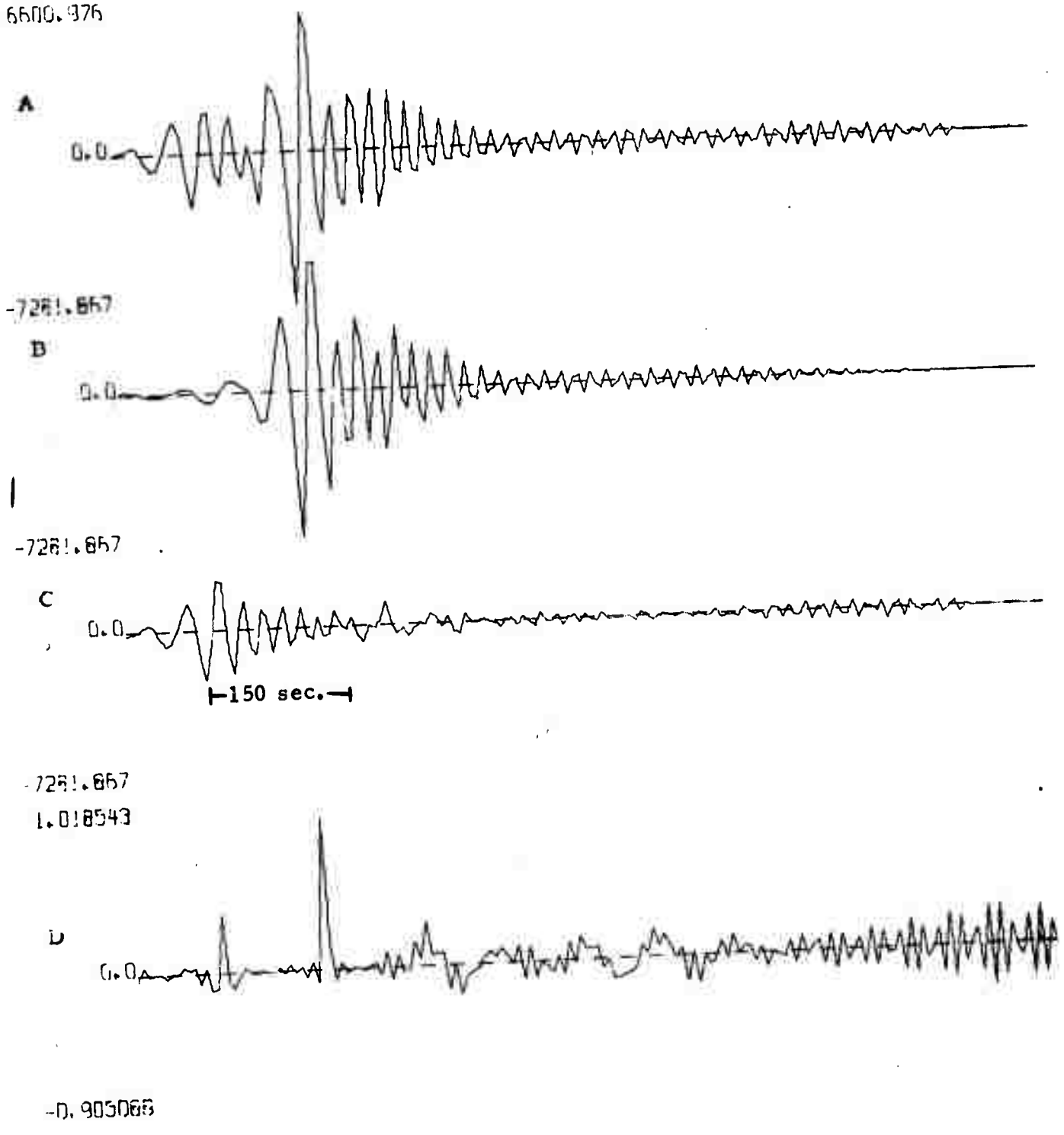

Trace D gives the multipath operator m(t). The two impluses mark the arrival of the two wavetrains separated by 108 seconds. It also shows that the Rayleigh wave amplitude of the first earthquake is about half of the second one. It is interesting to note that the difference in origin times of 108 seconds indicated by Trace D is exactly the same as that given by the PDE.

Since the two wavetrains are relatively free of multipath interference, the half-width of each impulse of m(t) is smaller than 10 seconds. This implies that successive events occurring as little as 20 seconds apart could be separated in cases where no multipathing occurs.

Figure 2 shows the corresponding data on frequency domain. The ordinate is expressed in digital units (counts)/Hz and the spectra are not corrected for instrument response. The dashed curve shows the amplitude spectral density of the original waveform (Trace A in Figure 1), the solid curve gives the corresponding amplitude spectrum of the isolated primary waveform (Trace B in the same figure). Note that the spectral modulation due to interference of the two successive wavetrains has been essentially completely removed by the complex cepstrum technique. The regularity of the spectral modulation is a strong indicator that the interference is caused by multiple events but not by multipath propagation.

Figure 3 gives another example of application of the complex cepstrum technique to a long wavetrain consisting of Love waves from two earthquakes at the same epicenter in the Kirgiz-Sinkiang border region reocrded at Chiangmai (CHG). PDE gives the following source parameters for these events:

Event 1	71-03-24	20:54:28.6	41.5N	79.5E	5.3 (m_b)
Event 2	71-03-24	21:01:54.9	41.4N	79.4E	5.3 (m_b)

Trace A shows the original Love waveform and Trace B gives the primary waveform recovered by the complex cepstrum technique. Trace C is the difference between Trace A and Trace B. The multipath operator is shown on Trace D. Again, the technique is able to separate the two events. However, the

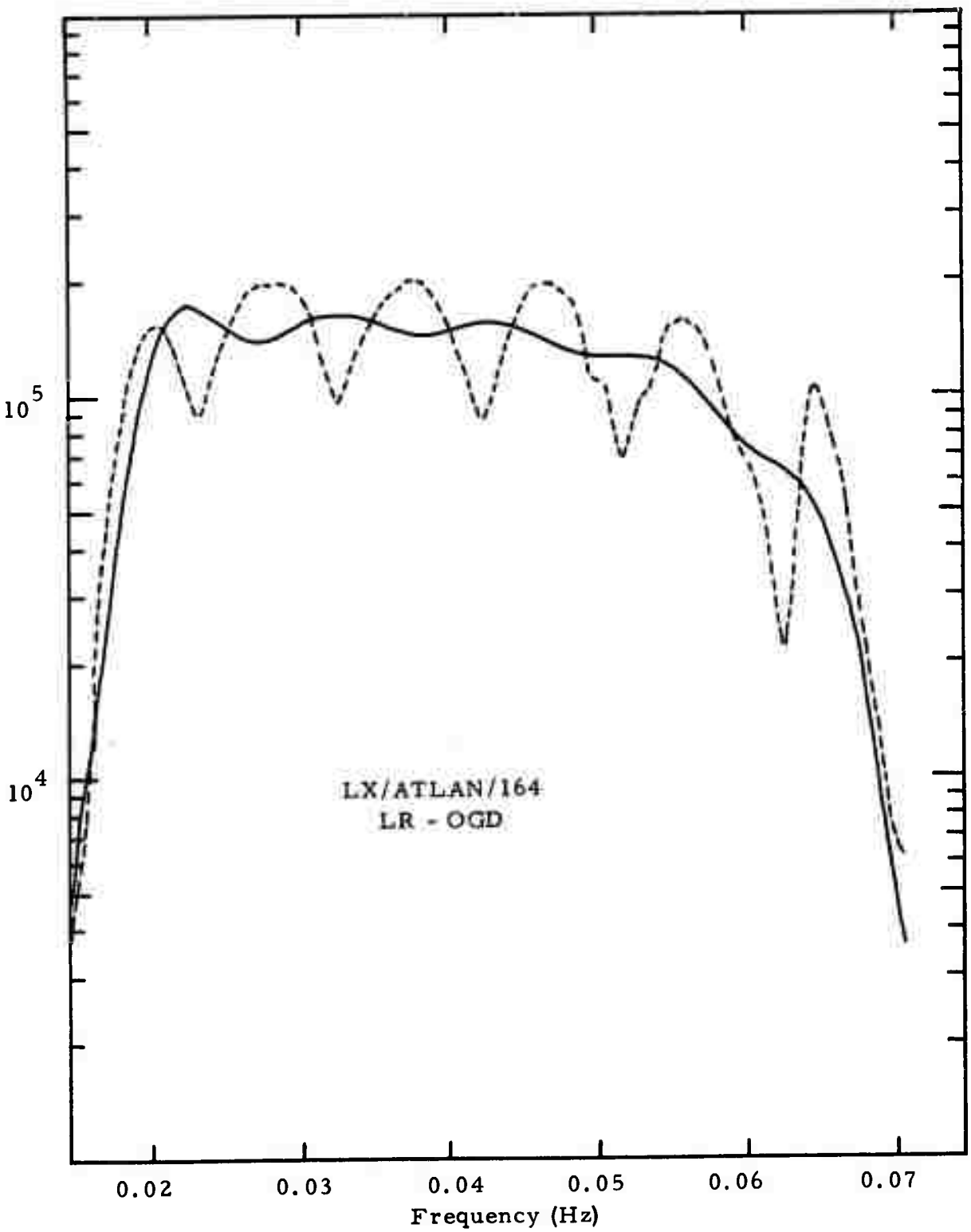

FIGURE 2

Fourier amplitude spectra of Rayleigh waves before and after application of the complex cepstrum technique. The dashed and solid curves represent spectra of Trace A and Trace B in Figure 1, respectively.

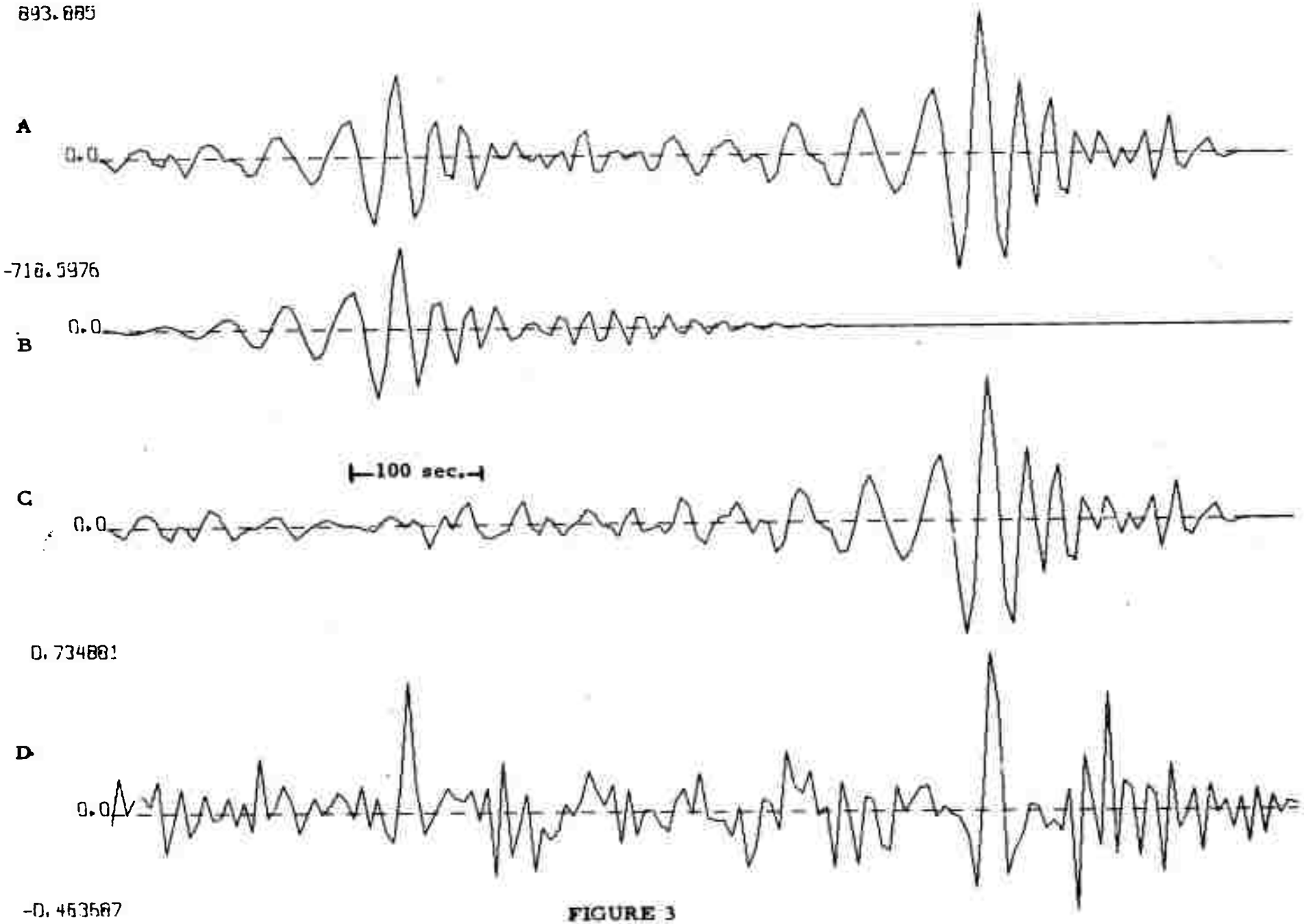

FIGURE 3

Results of application of the complex cepstrum technique. A. - Love waves from two earthquakes in the Kirgiz-Sinkiang border region recorded at CHG; B. - Love waves of the first earthquake recovered from Trace A by the

multipath operator is considerably more complicated than it was for the previous case. The two main impulses again indicate correctly the time delay between the earthquakes. In addition, there are high-frequency components of considerable amplitude indicating the presence of multipath propagation for each event.

Figure 4 shows the same example in frequency domain. The dashed curve represents the amplitude spectrum of the original waveform (Trace A of Figure 3). The solid curve shows the spectrum of the recovered waveform of the first earthquake (Trace B of Figure 3). Two points may be made of this figure. First, the periodicity of the spectral modulation is more rapid than for the previous example. This is because the time delay between the two events is about four times longer for the present case (the periodicity is inversely proportional to the time delay). Superimposed on this rapid modulation is a slower oscillation which is due to multipath propagation. The end result is a highly complicated spectrum which would probably deter any attempt to use it for source study without application of the complex cepstrum technique. The second point is that, as shown by the "clean-up" spectrum of the first earthquake (solid curve of Figure 4)the complex cepstrum technique can remove simultaneously the interference of multiple events and the interference of multipath propagation related to each of the individual events. This capability makes application of the technique straightforward.

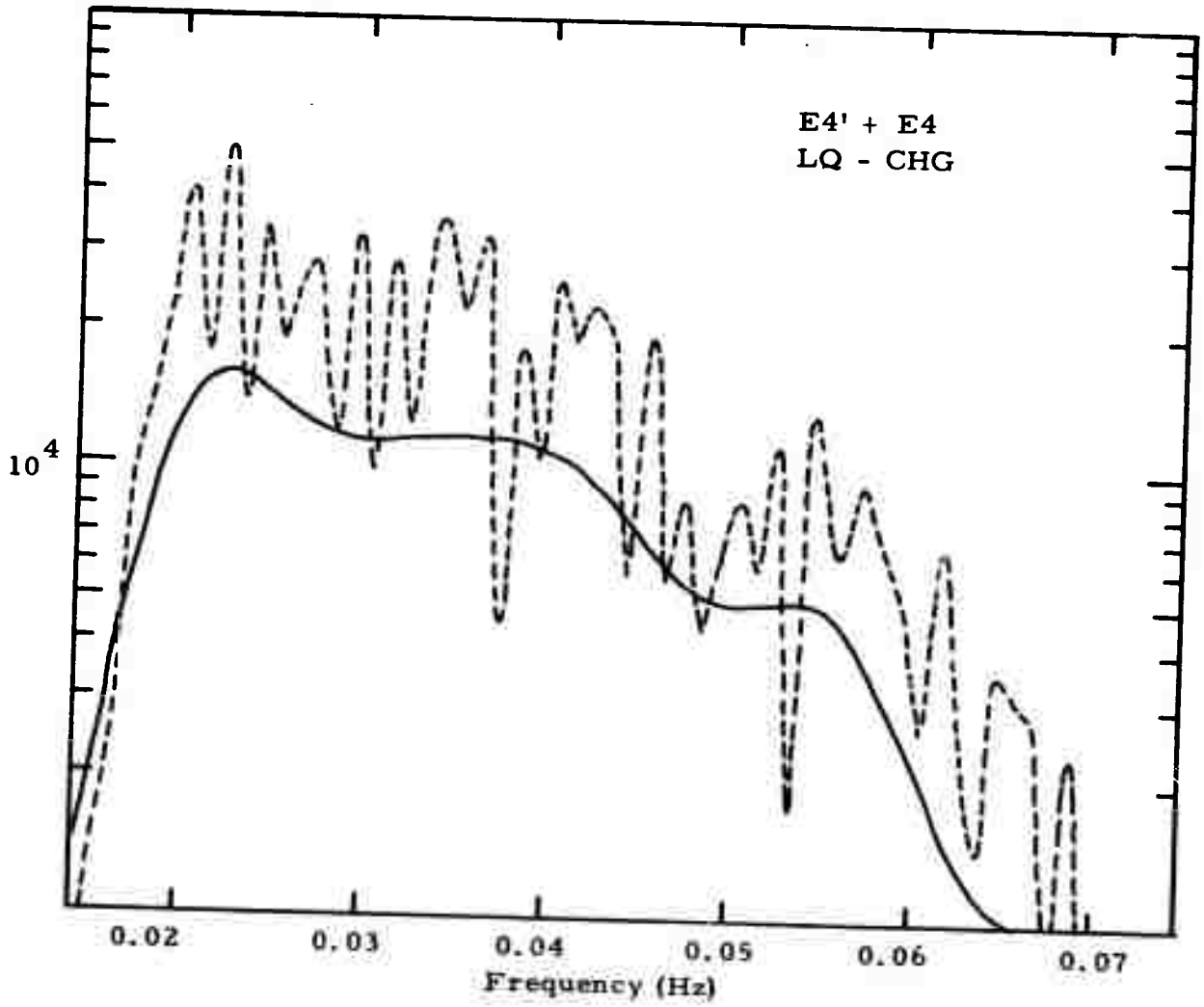

FIGURE 4

Fourier amplitude spectra of Love waves before and after application of the complex cepstrum technique. The dashed and solid curves represent spectra of Trace A and Trace B in Figure 3, respectively.

III. SURFACE WAVE SPECTRAL ANALYSIS ON A REGIONAL BASIS

It is known that the source mechanism of earthquakes and the structure of the crust and upper-mantle may vary from region to region. Thus, it becomes highly desirable from the standpoint of discrimination to compare surface wave spectra of seismic events on a regional basis. Furthermore, we are primarily concerned with medium to low magnitude seismic events. The surface waves generated by these shocks often are recorded with good quality only by seismograph stations not excessively far away from the epicenters. Thus, a regional analysis of surface wave spectra is also a practical necessity if these spectra are to be used to extract information about the source characteristics of relatively small seismic events. Surface wave spectra analyzed in this manner are potentially useful not only because they provide diagnostic criteria of their own for seismic discrimination, but also because they may provide explanations for anomalous Ms:m_b observed for a few events. Love waves are no less useful than Rayleigh waves in this regard. Therefore, whenever the data permit, we have analyzed both types of surface waves.

In the past six months amplitude spectra recorded at selected LPE stations have been computed and analyzed for Rayleigh and Love waves from 28 1971 seismic events. Of the 28 events 11 are located in the Arctic Ocean and the remaining 17 are located in the Eurasian continent ranging from Turkey in the west to Yunnan Province, China in the east. Table 1 lists the detailed information on epicenter , origin time and magnitude of these events as given by PDE. A map showing the locations of these seismic events and two recording sites, CHG and EIL is given in Figure 5. In terms of source classification, two of 28 events are presumed underground nuclear explosions in Novaya Zemlya. The remaining 26 events are earthquakes with magnitudes (m_b) ranging from 4.5 to 5.4, except for one m_b= 6.0 event. We now present the spectra of Rayleigh and some Love waves for these seismic events on a regional basis.

No.	Date	Time	Latitude	Longtitude	Depth	m_b	Sites
A1	71-10-14	05:59:57.1	73.3N	55.1E	0	6.7	FBK
A2	71-09-27	05:59:55.0	73.4N	55.1E	0	6.4	OGD
A3	71-08-22	11:07:21.0	83.0N	6.5W	N	4.6	OGD
A4	71-01-27	20:45:42.8	76.7N	7.0E	31	4.9	FBK, OGD
A5	71-01-29	08:33:49.7	78.8N	8.0E	N	4.8	FBK, OGD
A6	71-01-28	11:03:49.5	76.5N	8.1E	N	4.5	FBK, OGD
A7	71-01-31	04:33:27.4	76.6N	7.3E	N	4.7	FBK, OGD
A8	71-01-26	08:08:44.1	77.1N	8.5E	N	4.6	FBK, OGD
A9	71-06-04	09:10:03	84.6N	108.0E	N	5.1	OGD
A10	71-08-21	19:34:23	81.9N	118.9E	N	4.6	OGD
A11	71-06-04	07:56:55	84.5N	107.5E	N	5.0	OGD
B1	71-01-26	22:48:31.1	43.8N	39.2E	28	4.8	EIL
B2	71-04-17	16:37:38	41.0N	37.0E	N	4.8	EIL
B3	71-05-24	02:20:14	38.8N	40.5E	N	4.7	EIL
C1	71-06-08	16:59:25	37.5N	29.8E	10	4.7	EIL
C2	71-06-04	15:06:12	37.6N	29.8E	27	4.6	EIL
C3	71-05-23	20:11:23	37.6N	29.9E	33	4.7	EIL
D1	71-04-06	06:49:52	29.8N	51.9E	10	5.2	EIL
D2	71-03-31	20:47:13	34.6N	50.3E	31	4.4	EIL
D3	71-05-22	14:02:07	35.6N	58.3E	36	4.8	EIL
D4	71-01-28	15:51:06.6	35.0N	47.0E	43	4.6	EIL
E1	71-05-27	00:30:28	38.3N	69.0E	36	4.8	EIL
E2	71-04-04	01:35:23	38.4N	73.3E	33	4.8	EIL, CHG
E3	71-03-23	20:47:17	41.5N	79.3E	33	6.0	CHG
E4'	71-03-24	20:54:29	41.5N	79.5E	18	5.3	CHG
E4	71-03-24	21:01:55	41.4N	79.4E	25	5.3	CHG
E5	71-05-03	00:33:22	30.8N	84.5E	16	5.4	CHG
E6	71-06-04	14:10:46	32.2N	95.2E	N	5.0	CHG
E7	71-02-05	09:10:35.7	25.2N	99.4E	N	5.3	CHG

TABLE 1

The origin time, location, and magnitude of the seismic events studied.

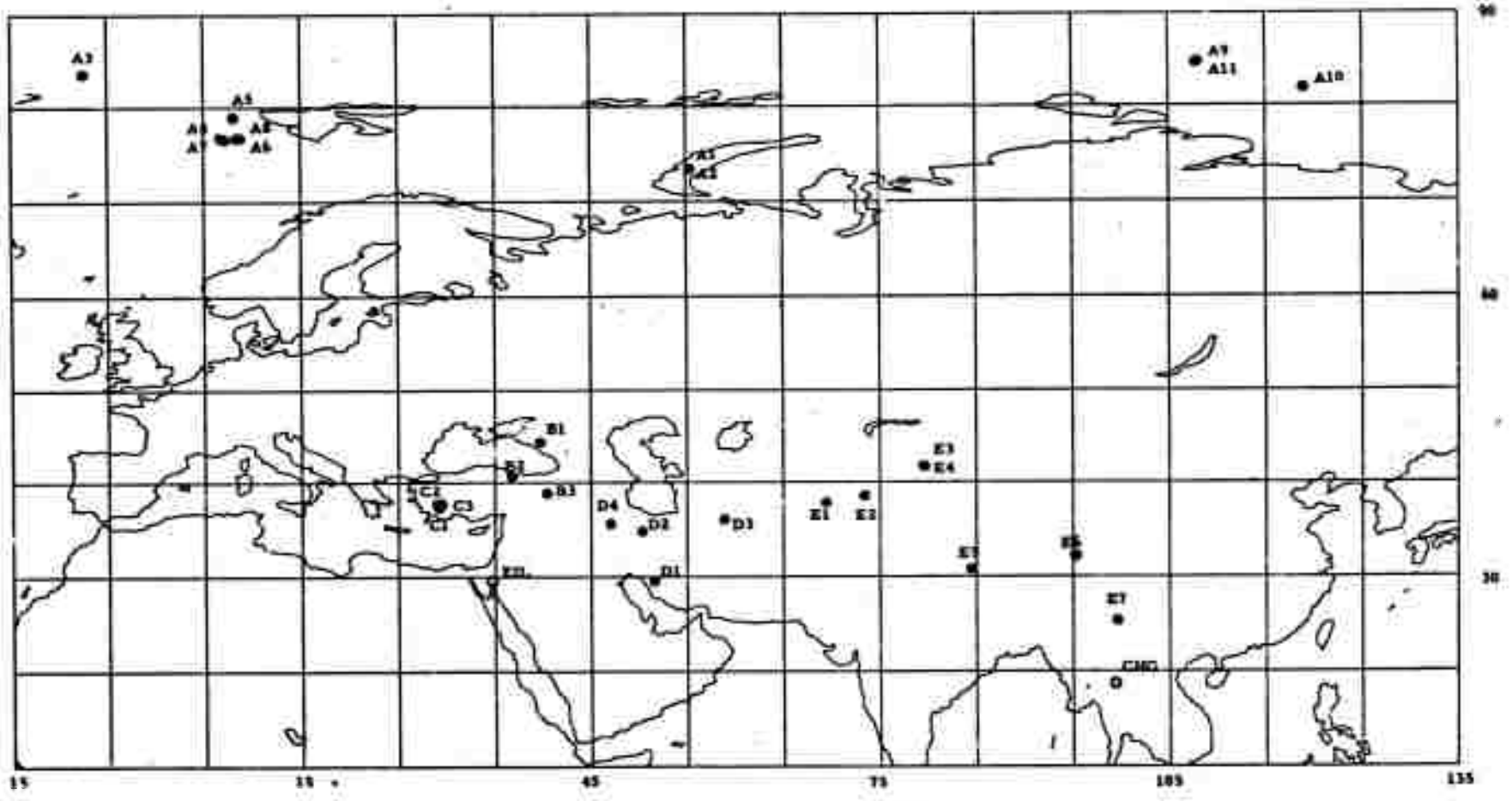

MAP SCALE: 1.000 IN./ 10 DEG. LONGITUDE

FIGURE 5

Locations of the seismic events listed in Table 1 and the recording sites CHG, EIL.

(a) Earthquakes and Explosions in the Arctic Ocean

Rayleigh wave spectra are obtained for two underground nuclear explosions (Events A1 and A2) in Novaya Zemlya, six earthquakes (A3 through A8) in the Spitsbergen fracture zone extending north-westward from the Svalbard Island region and three earthquakes (A9 through A11) in the Arctic ridge near Severnaya Zemlya. These spectra are shown in Figure 6. The spectral density is expressed in the quantum units (counts)/Hz and are uncorrected for system response. The spectra on the left side of the figure are from FBK (Fairbanks, Alaska), those on the right side are from OGD (Ogdensburg, New Jersey). The instrumental response is essentially the same for these two sites except that OGD magnification is higher.

On the basis of these spectra the following remarks can be made.

(1) Rayleigh waves generated by the two underground nuclear explosions in Novaya Zemlya as recorded at FBK for Event A1 and at OGD for Event A2 have very similar spectral content, increasing by a factor of about 10 from 0.02 to 0.04 Hz. In addition, the absolute spectral levels for the two events are consistent with their m_b values, even though the spectra are obtained at two different azimuths from the source. These observations suggest that Rayleigh wave spectra for underground nuclear explosions in Novaya Zemlya may be repeatable from event to event and may be independent of azimuth.

(2) Rayleigh wave spectra for the earthquakes near Svalbard Island (Events A4 to A8) have similar shapes for any given event at OGD and FBK, even though the azimuths to these stations differ by about 60°. On the other hand, the spectral shape may change notably from event to event (compare A4 and A5), even though their epicenters are located near one another. The absolute spectral level at OGD is about three times the level at FBK for the five events recorded at both stations. These observations imply that all events have the same type of source mechanism and the difference in spectral shapes among events probably is due to differences in focal depth. (Tsai and Aki 1970).

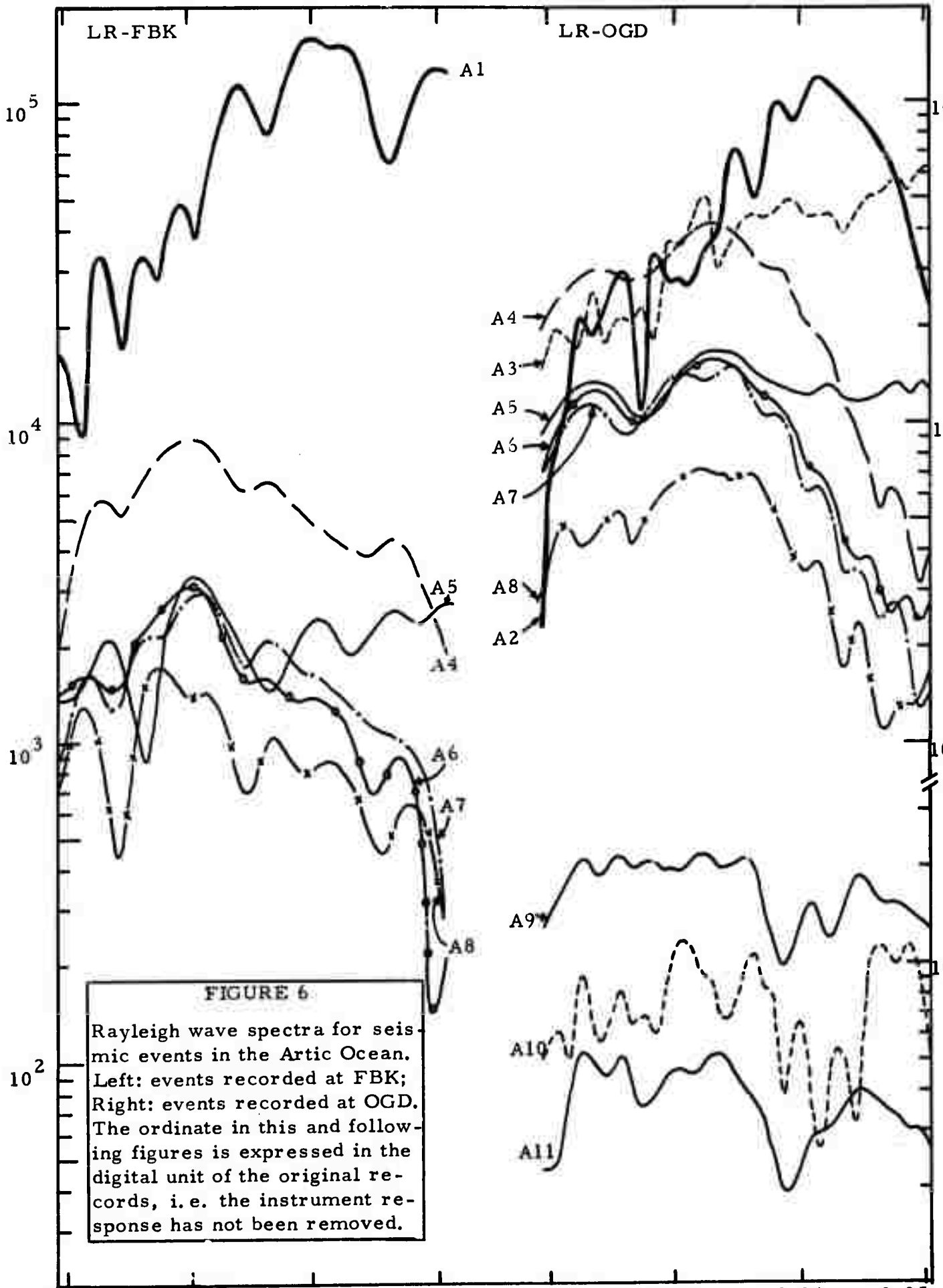

FIGURE 6

Rayleigh wave spectra for seismic events in the Artic Ocean. Left: events recorded at FBK; Right: events recorded at OGD. The ordinate in this and following figures is expressed in the digital unit of the original records, i.e. the instrument response has not been removed.

Furthermore, the factor of three difference in spectral levels between OGD and FBK is consistent with a transform fault mechanism striking in the same general direction as the Spitsbergen fracture zone. Thus, we tentatively conclude that the five earthquakes studied here have similar transform fault source mechanisms. This type of mechanism has been observed by Sykes (1967) for earthquakes in many other fracture zones over the world.

(3) The spectra of Rayleigh waves are very similar in general shape for the three earthquakes (A9, A10, A11) near Severnaya Zemlya as observed at OGD. Since our data are limited to Rayleigh waves at one station, no statement about possible source mechanisms for these earthquakes can be made at present.

(4) Rayleigh waves from the presumed underground nuclear explosions in Novaya Zemlya differ substantially from eight of the nine earthquakes in the Arctic Ocean studied here in that they have greater amplitudes in the frequency range of 0.04 to 0.05 Hz. The ninth earthquake (Event A3) appears to generate Rayleigh waves having a spectral shape similar to that of the presumed explosions. Tsai and Aki (1971) pointed out that, while a great many earthquakes can be discriminated against underground nuclear explosions using Rayleigh wave spectra, there likely will be a small number of earthquakes which can not be identified by this criterion. Our observations here appear to confirm above statement, which was made on theoretical grounds. Note, however, that we have only Rayleigh wave spectra at just two stations; it may have been possible to identify Event A3 if the Love waves and/or additional stations had been available. Also, Event A3 still can be positively discriminated from Event 2 using $M_s:m_b$.

(b) Earthquakes in Caucasus and Eastern Turkey

Event B1 is an earthquake in western Caucasus and Events B2, B3 are two earthquakes in Eastern Turkey. The amplitude spectra of Rayleigh waves from all the three events and those of Love waves from two of the three

events, as observed at EIL (Eilat, Isreal), are shown, respectively, on the left and right sides of Figure 7. The dashed and solid curves for each event are the spectra before and after application of the complex cepstrum technique, respectively. The Rayleigh wave spectra of the three earthquakes differ from each other notably, but the Love wave spectra appear to be more predictable. More detailed interpretation of the spectra for Events B2 and B3 will be given later in Section IV.

(c) Earthquakes in Southwestern Turkey

Rayleigh wave spectra from EIL for three aftershocks (Events C1, C2, C3) of an m_b=5.5 earthquake, which occurred on May 12, 1971 in Southwestern Turkey are shown on the right side of Figure 8. The dashed and the solid curves are the spectra before and after application of the complex cepstrum technique. As seen from the figure all three spectra are virtually identical in shape and marked by a deep spectral minimum at about 0.045 Hz. Since the path from the epicenter to the recording site EIL is complicated (a large segment is across the eastern Mediterranean Sea), it is not possible on the basis of one station to determine whether the spectral minimum is caused by source effects or propagation effects.

(d) Earthquakes in Iran

Rayleigh wave spectra for four earthquakes in Iran (Events D1, D2, D3 and D4) as observed at EIL are shown on the left side of Figure 8. The four spectra are again quite varied in their shapes even though the propagation paths are quite similar. Thus, it can be said that such spectral differences most likely reflect the differences in source mechanism and/or focal depth. Unfortunately, the N-S component of the digital records in this time period is unusable, so we do not have corresponding Love wave spectra for most of the events discussed here.

(e) Earthquakes in Central Asia, Tibet and Southwestern China

Rayleigh and Love wave spectra for seven earthquakes recorded at CHG (Chiangmai, Thailand) and EIL are shown in Figures 9, 10, and 11.

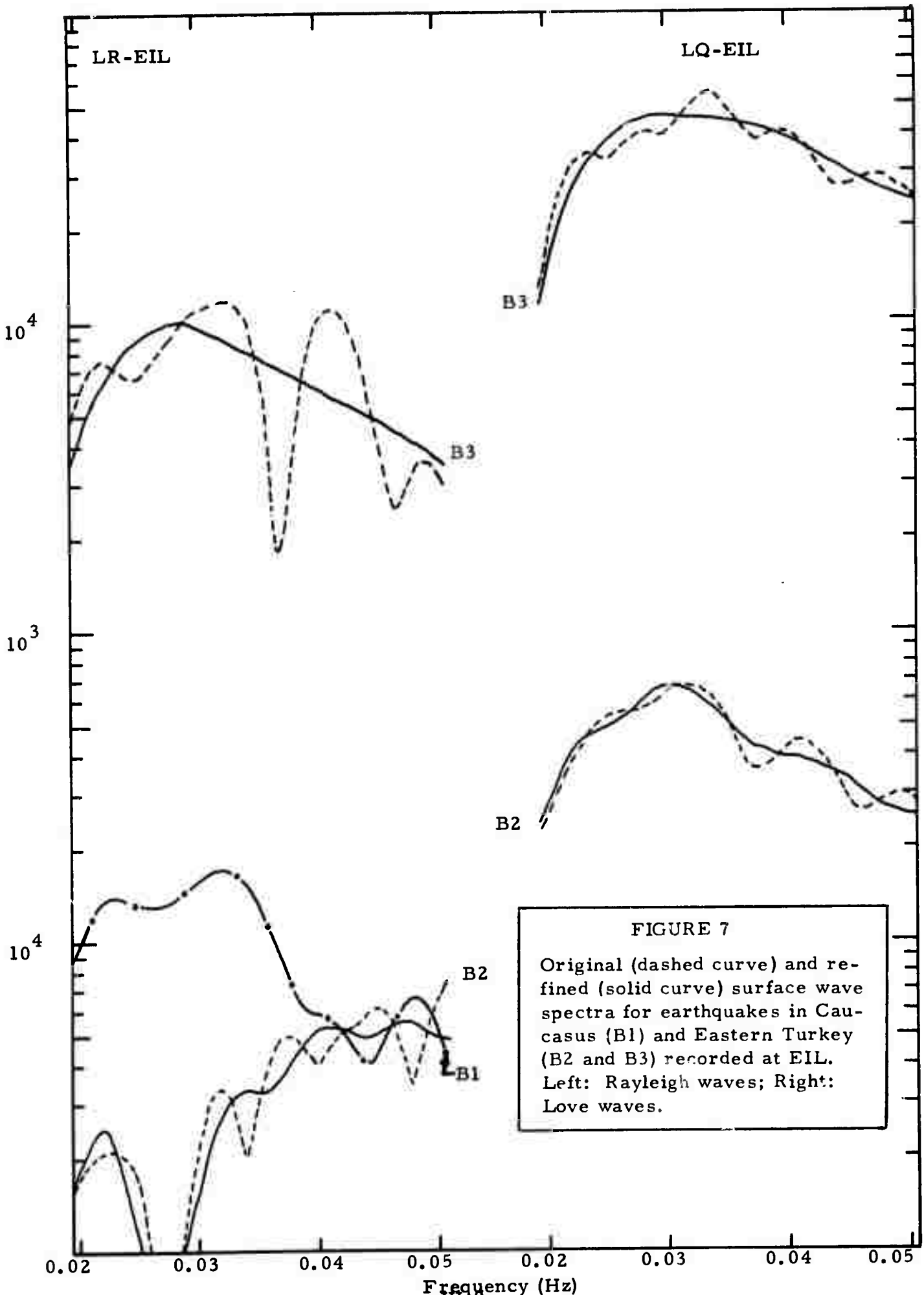

FIGURE 7

Original (dashed curve) and refined (solid curve) surface wave spectra for earthquakes in Caucasus (B1) and Eastern Turkey (B2 and B3) recorded at EIL. Left: Rayleigh waves; Right: Love waves.

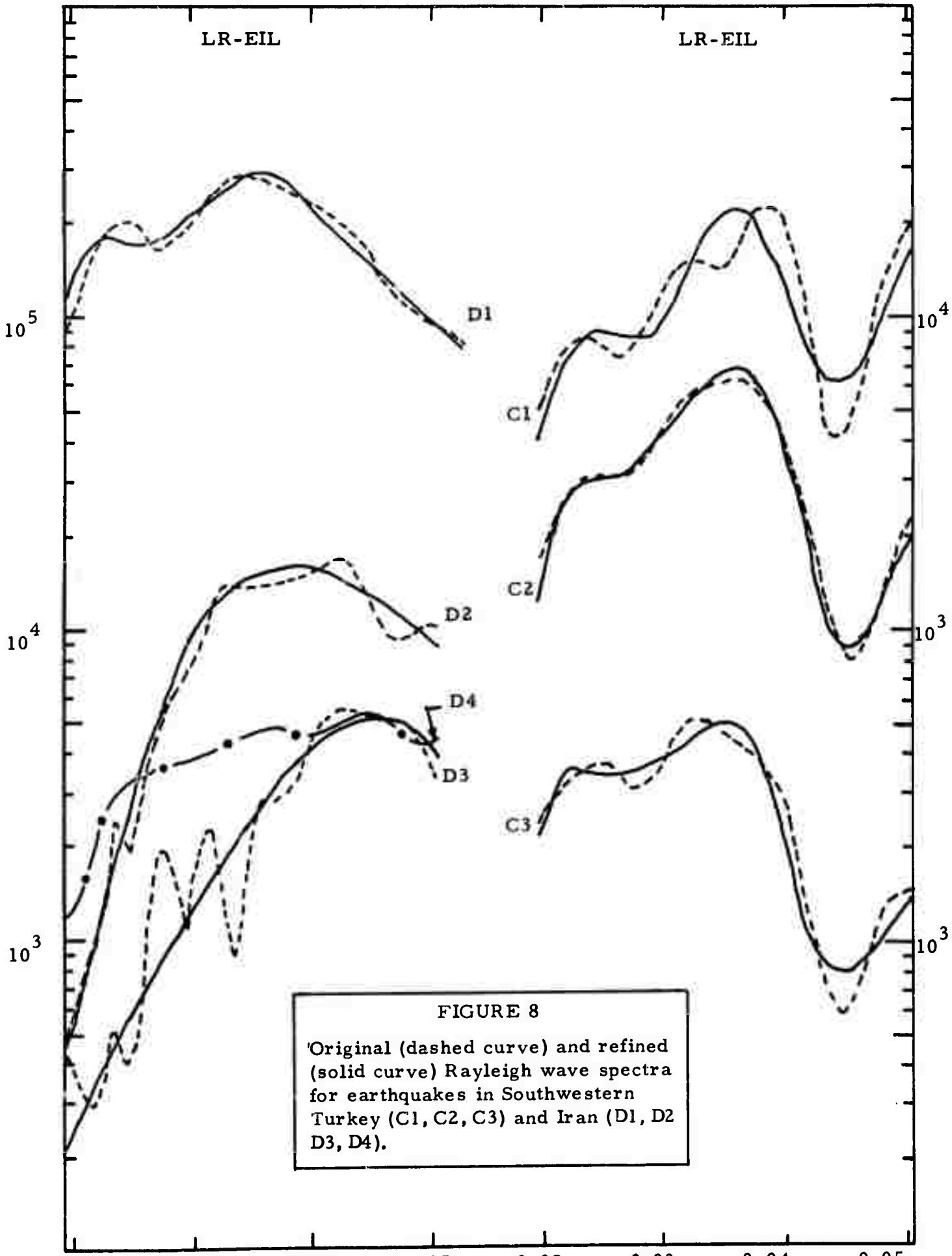

FIGURE 8

Original (dashed curve) and refined (solid curve) Rayleigh wave spectra for earthquakes in Southwestern Turkey (C1, C2, C3) and Iran (D1, D2 D3, D4).

Event E1 is an earthquake in Tadzhik, USSR. The observed EIL Rayleigh and Love wave spectra of this earthquake are given in the lower part of Figure 9. The spectral level of Rayleigh waves is nearly three times that of Love waves at the same site. Thus, EIL appears to be in the nodal direction of Love wave radiation for this earthquake.

Event E2 is an earthquake located in the Tadzhik-Sinkiang border region and its Rayleigh wave spectra at CHG and EIL are shown in the upper part of the left side of Figure 9. The corresponding Love wave spectrum at CHG is given in the upper part of the right side of the same figure. The dashed and the solid curves in the figure denote the spectra before and after application of the complex cepstrum technique, respectively. It can be seen from the observed data in this figure and two figures to follow that multipath propagation often is present in both Rayleigh and Love waves even though the propagation path is entirely within the continent. Further interpretation of these spectra will be given in Section IV.

Figure 10 shows Rayleigh and Love wave spectra obtained at CHG for two earthquakes (Events E3 and E4) located at the same epicenter in the Kirgiz-Sinkiang border region. The two earthquakes generate virtually identical Rayleigh and Love wave spectra even though the spectral level of Event E3 is about 20 times the level of Event E4. This phenomenon was observed earlier for the three smaller earthquakes in Southwestern Turkey (Events C1, C2 and C3). Incidentally, Event E4 here is the second one of the two events on Trace A of Figure 3 shown in the discussion of the complex cepstrum technique (Section II), and its refined Love wave spectrum obtained here (solid curve on the lower - right corner of Figure 10) is nearly identical to that of the first event obtained earlier (solid curve in Figure 4).

Comparison of the spectra between Event E2 on the one hand and Events E3 and E4 on the other hand indicates that Rayleigh waves are entirely different in spectral shape while Love waves are very similar. Further interpretation of the spectra for Events E3 and E4 is given in Section IV.

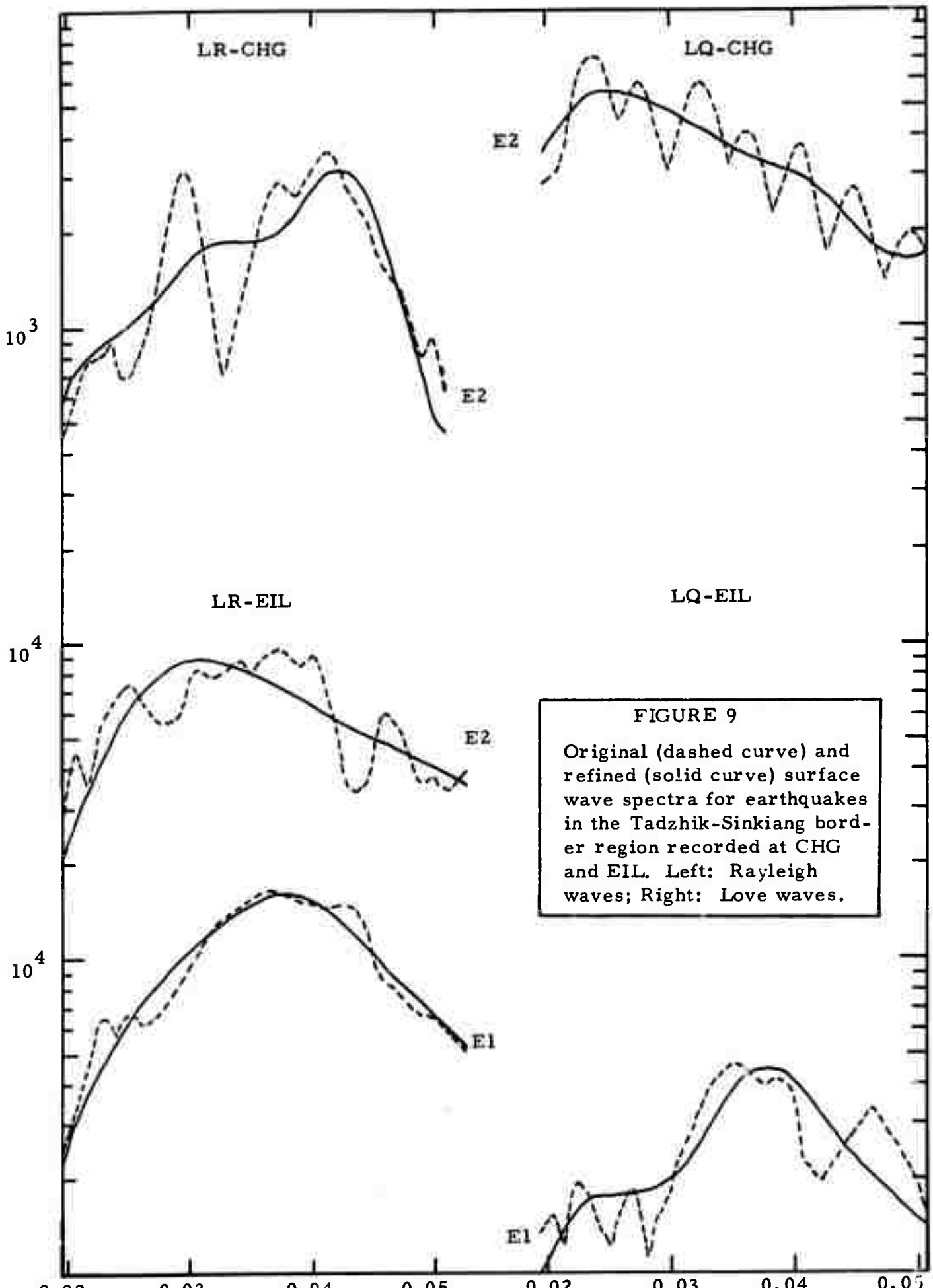

FIGURE 9

Original (dashed curve) and refined (solid curve) surface wave spectra for earthquakes in the Tadzhik-Sinkiang border region recorded at CHG and EIL. Left: Rayleigh waves; Right: Love waves.

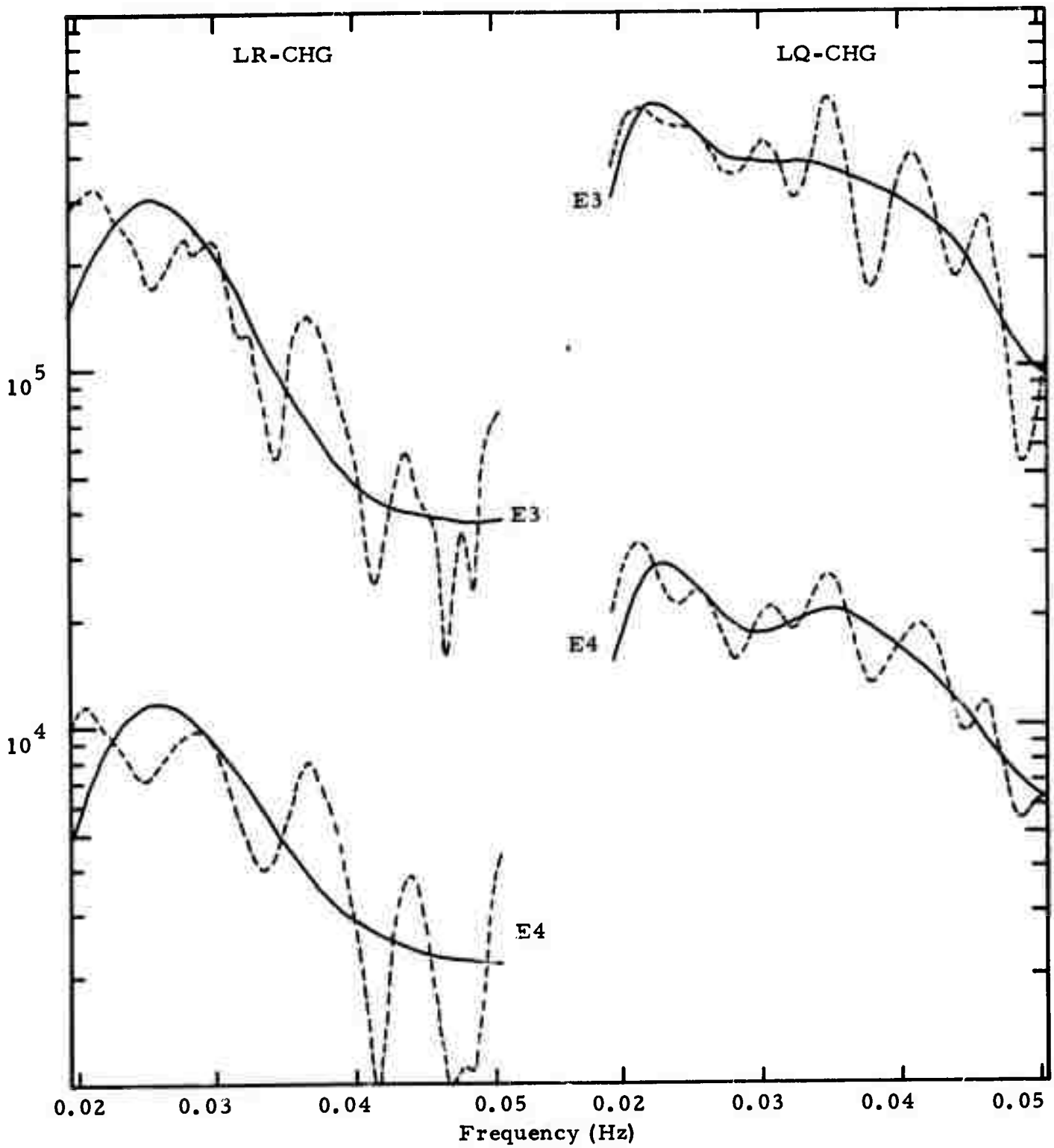

FIGURE 10

Original (dashed curve) and refined (solid curve) surface wave spectra for two earthquakes in the Kirgiz-Sinkiang border region recorded at CHG. Left: Rayleigh waves; Right: Love waves.

Figure 11 shows Rayleigh and Love wave spectra from CHG for Events E5 and E6, two earthquakes located in Tibet. The Rayleigh wave spectrum for a third earthquake in Yunnan Province, China (Event E7) also is given in the figure. As seen earlier, the observed Rayleigh wave spectra differ greatly from each other whereas the spectral shape of Love waves changes very little from event to event. In fact, the five observed Love wave spectra from Events E2, E3, E4, E5 and E6 have almost identical spectral shape even though their epicenters cover a wide geographical area.

Based on the observational evidence presented above the following remarks about the spectral behavior of surface waves from seismic events in the Arctic Ocean and the Eurasian Continent can be made.

(1) Rayleigh wave spectra from underground nuclear explosions in Novaya Zemlya appear to have the same spectral shape from event to event and vary very little with azimuth. Furthermore, these spectra are substantially different from those of a great majority of earthquakes in the neighboring seismic areas such as Svalbard Island region and Severnaya Zemlya region.

(2) The spectral shapes of both Love and Rayleigh waves appear to remain unchanged from event to event for events located at the same epicenter. This phenomenon may enable us to establish a relatively stable library of master surface wave spectra. These master spectra can subsequently be used to monitor changes in source characteristics that may accompany future seismic events taking place at the epicenters of these master surface wave spectra.

(3) The spectral shapes of Love waves from earthquakes located in a wide variety of geographical areas in Central Asia, Tibet and Southwestern China appear to vary very little from event to event. On the contrary, Rayleigh wave spectral shapes vary greatly among earthquakes from one epicentral region to another. Although it is possible that such a phenomenon may be caused by differential effects of propagation, it is far more likely that the phenomenon is a direct result of different source mechanisms and/or focal depths (as predicted by theory). Consequently, the large variation of Rayleigh wave spectra

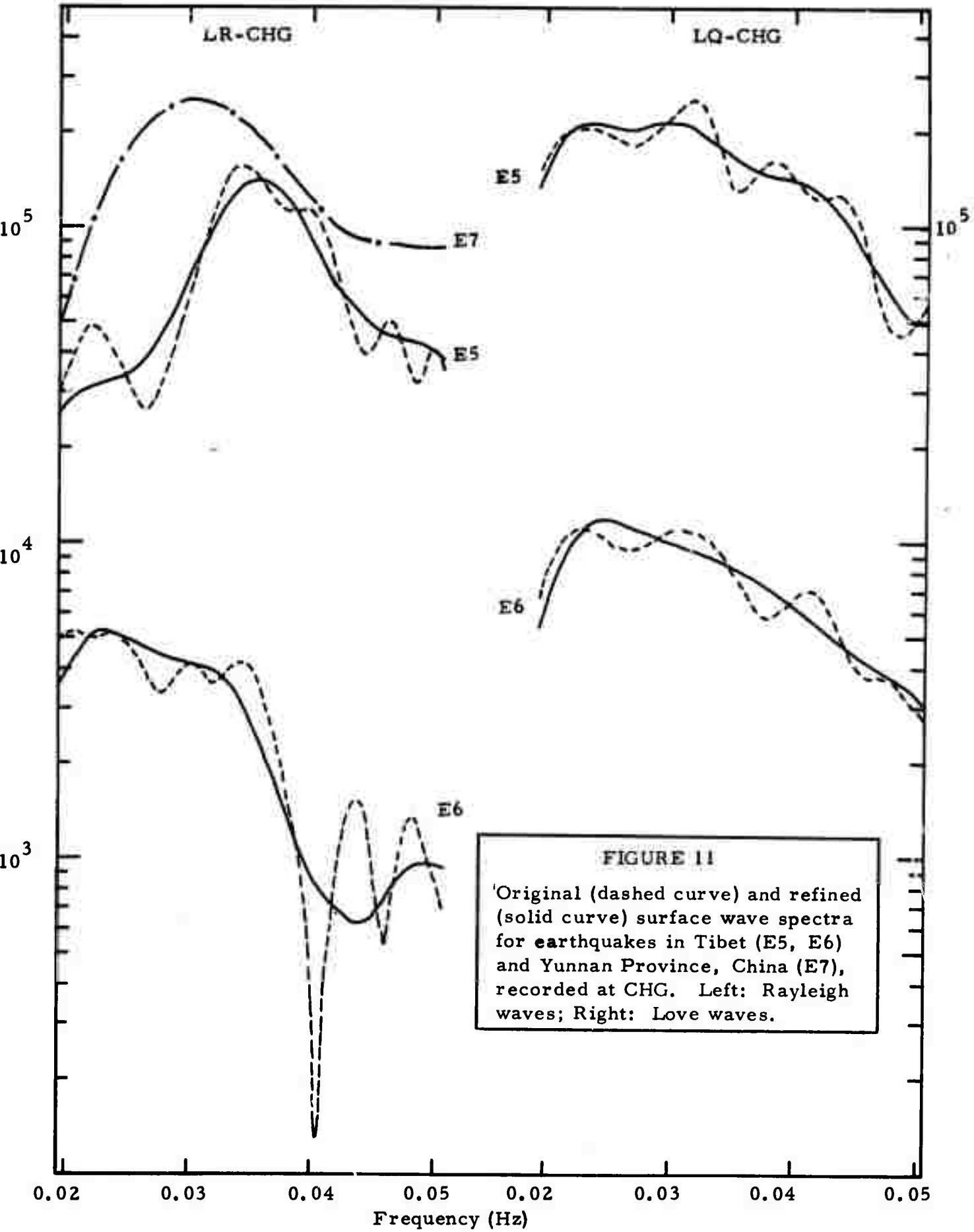

FIGURE 11

Original (dashed curve) and refined (solid curve) surface wave spectra for earthquakes in Tibet (E5, E6) and Yunnan Province, China (E7), recorded at CHG. Left: Rayleigh waves; Right: Love waves.

among seismic events can be exploited for the discrimination purpose. Meanwhile, Love wave spectra can be used as an additional important yardstick for measuring the azimuthal dependence of radiation patterns.

It should be pointed out that the foregoing remarks have been drawn from a relatively small ensemble of earthquakes. As data accumulate, these remarks may be refined or even revised.

IV SOURCE CHARACTERIZATION BY AMPLITUDE SPECTRA OF SURFACE WAVES

Our ultimate goal is to determine the source mechanisms and focal depths of seismic events using the amplitude spectra of surface waves. Two essential elements are involved in this problem, one theoretical and the other observational.

On the theoretical side of the problem, we start with a model for the elastic medium. Based on this prescribed earth's model, we can compute theoretical Rayleigh and Love wave spectra for a double-couple point source of an arbitrary orientation and at different depths from the surface by using Saito's method (Saito, 1967). For earthquakes, a step function in time is assumed to represent the history of source behavior.

Now we are provided with a set of observed Love and Rayleigh wave spectra from a seismic event and asked to determine the source mechanism and focal depth of the event. Thus, the problem of finding a theoretical source model from the given set of data is an inverse one. As many other inversion problems in geophysics, even the "best-solution" is inherently nonunique. We have used a simple least-squares error criterion for determining the best fit between the sets of observed and the theoretical spectra.

The amplitude spectra of Rayleigh and/or Love waves at a number of sites are obtained by using the fast Fourier transform technique. (The surface waveforms first are "demultipathed", if necessary, using the complex cepstrum technique described in Section II). The spectra then are corrected for individual instrument response and equalized to a common epicentral distance by multiplying a geometrical spreading factor. The processed spectra become the input of a searching routine designed to find a "best-fit" solution. In the process of searching a subroutine is called to compute a set of theoretical surface wave

spectra at the azimuths corresponding to the recording sites of the data used. Attached to each set of theoretical spectra is a set of source parameters consisting of the strike, the dip angle of the fault, the slip angle of the dislocation on the fault and the focal depth. The theoretical spectra then are compared with the corresponding observed spectra and an error count based on the sum of squares of residuals is kept for each theoretical model.

Let X_{ij}^R and X_{ij}^L denote the observed Rayleigh and Love wave spectra respectively, at j^{th} site and i^{th} frequency. Y_{ij}^R and Y_{ij}^L denote the corresponding theoretical spectra. The sum of the squares of residuals S is defined as

$$S = \sum_j \sum_i \left[(X_{ij}^R - C Y_{ij}^R)^2 + (X_{ij}^L - C Y_{ij}^L)^2 \right] \qquad (1)$$

The error count of S will be minimum for this particular set of Y_{ij}^R and Y_{ij}^L if

$$C = \frac{\sum_j \sum_i \left[X_{ij}^R \; Y_{ij}^R + X_{ij}^L \; Y_{ij}^L \right]}{\sum_j \sum_i \left[Y_{ij}^R \; Y_{ij}^R + Y_{ij}^L \; Y_{ij}^L \right]} \qquad (2)$$

For comparison between the observed and each set ot theoretical spectra, we first calculate the scalar factor C according to equation (2). This C value is subsequently inserted in equation (1) to yield an estimate of the error count S.

The four source parameters (strike, dip angle, slip angle and focal depth) are varied systematically so as to cover all conceivable combinations of their values. The error counts of two successive sets of source parameters are compared and the smaller one is retained along with the corresponding set of source parameters for the next comparison. The set of theoretical spectra which yield the minimum value of S is said to be the best-fit spectra and the corresponding source parameters are taken as the final solution of the source mechanism and focal depth.

We have tested this automatic searching scheme on a number of observed spectra given in the preceding section. In these tests we have used a

Gutenberg continental model of 38-km crust. The range and increment of the four source parameters are as follows:

	Range	Increment
Strike (ϕ)	0^o - 180^o	10^o
Dip angle (δ)	20^o - 80^o	20^o
Slip angle (λ)	0^o - 90^o	30^o
Focal depth (h)	0 - 100km	5 km

Note that we do not use $\delta = 90^o$ in order to avoid the presence of deep minima in the theoretical Rayleigh wave spectra which may inflate the error count S so much that an otherwise good source model with $\delta = 90^o$ will be disqualified. The results of these tests are described below.

Figure 12 shows the observed and the "best-fit" theoretical spectra for the two Eastern Turkey earthquakes, (Events B2 and B3). In the figure the dashed and the solid curves represent the observed and the theoretical spectra, respectively, at EIL. Note that the observed spectra shown are after correction for system response and geometrical spreading.

For Event B2 the source parameters corresponding to the theoretical spectra shown in the figure are ϕ = N130°E, $\delta = 80^o$, $\lambda = 0^o$ and h=38km. In other words, the source mechanism of this earthquake is a strike-slip fault on a nearly vertical plane and striking in the direction of N 130°E. The focal depth is determined as 38 km. This is consistent with the dislocation of the Anatolia Fault on which the epicenter of this event is located.

For Event B3 the "best-fit" theoretical spectra for the data obtained at EIL as shown in the lower part of Figure 12 corresponds to a focus having following fault-plane parameters: A. ϕ = N 20°E, $\delta = 80^o$, $\lambda = 0^o$, and h = 14 km (or B. ϕ = N110°E, $\delta = 90^o$, $\lambda = 10^o$, and h = 14 km. (Note that Plane A and Plane B are mutually orthogonal). Canitez and Toksoz (1971) have studied an earthquake taken place at this area on July 26, 1967 using both body and surface wave data and obtained the following parameters: ϕ = N101°E, $\delta = 94^o$, $\lambda = 16^o$ and h = 12 km. Thus our Plane B for Event B3 is very consistent with their result. This cross check suggests that the automatic searching scheme using both Rayleigh and Love wave spectra simultaneously at a few sites is capable of yielding

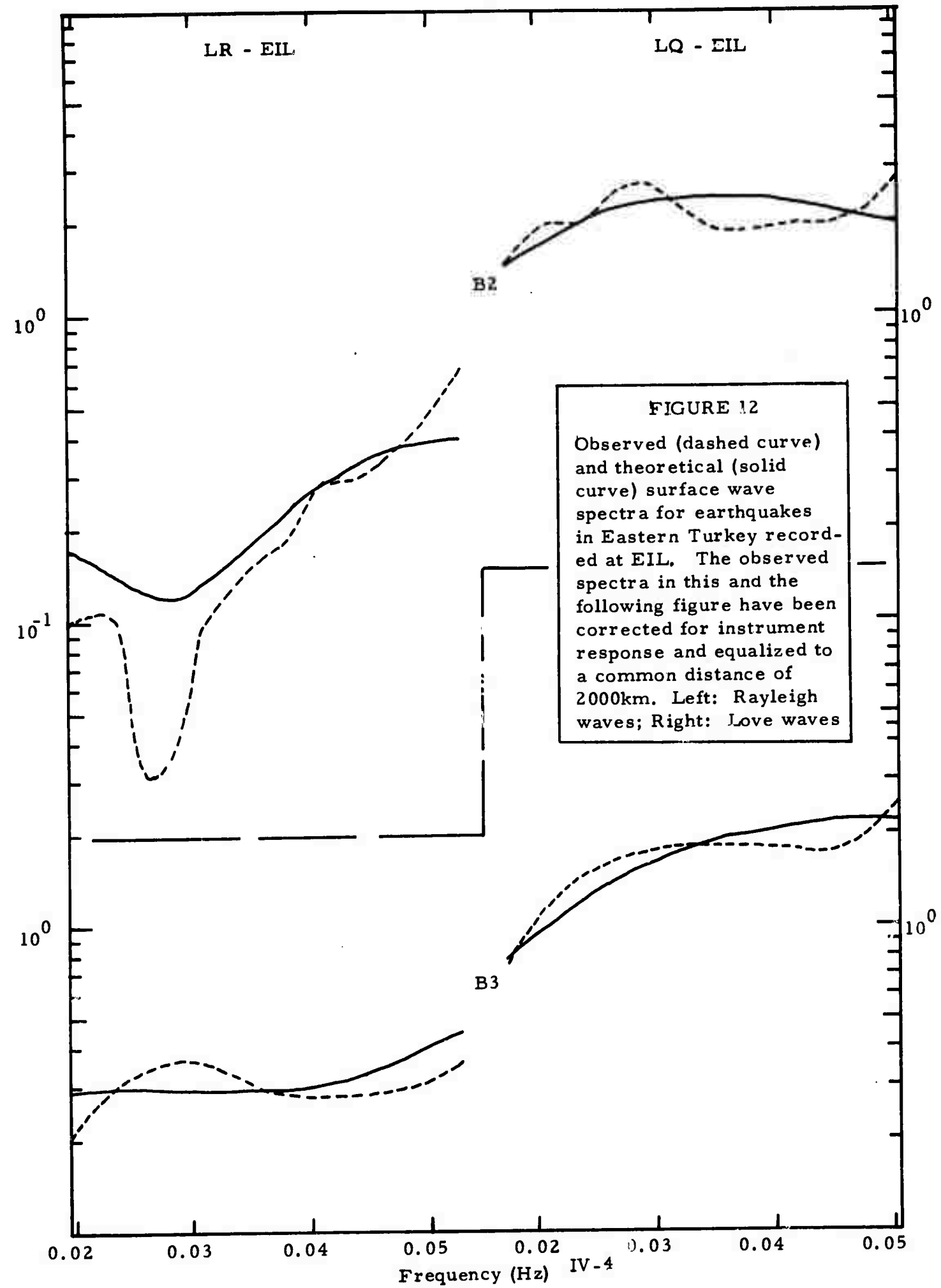

FIGURE 12

Observed (dashed curve) and theoretical (solid curve) surface wave spectra for earthquakes in Eastern Turkey recorded at EIL. The observed spectra in this and the following figure have been corrected for instrument response and equalized to a common distance of 2000km. Left: Rayleigh waves; Right: Love waves

correct estimates of some source parameters if the structure can be represented adequately by a flat-layered earth model.

Figure 13 shows the results of applying the automatic searching scheme to the data of three Central Asian earthquakes (Events E2, E3 and E4). Again, the dashed and the solid curves in the figure represent the observed and the "best-fit" theoretical spectra.

For Event E2 we have Rayleigh wave spectra available at CHG and EIL plus Love wave spectra available at CHG only. Because of the uncertainty on the relative magnification level between the two stations we have started with the data at CHG alone. The solution is then checked on the data at EIL. The results are shown on the upper part of Figure 13. The source parameters obtained give the following values: ϕ = N120°E, δ = 60°, λ = 60°, h = 44 km. The source mechanism is in good agreement with the fault-plane solutions obtained for several earthquakes in the same epicentral region by Shirokova (1967).

Events E3 and E4 are two earthquakes having the same epicenter in the Kirgiz-Sinkiang border region. The observed Rayleigh and Love wave spectra are obtained at CHG. The "best-fit" theoretical spectra gave the following source parameters: ϕ = N70°E, δ = 20°, λ = 0°, h = 55 km for Event E3; ϕ = N70°E, δ = 20°, λ = 0°, h = 50 km for Event E4. The source mechanism defined by the preceding parameters would give a low angle strike-slip fault which seems unlikely for these earthquakes. Thus, a plane orthogonal to this plane is more likely to be the fault plane of these two earthquakes, namely, the plane with the following parameters: ϕ=N160°E, δ = 90°, λ = 70°. If this is indeed the case, then the source mechanism of these earthquakes would correspond to a normal fault on a vertical plane. However, this interpretation should be taken as tentative for the following reasons:

(1) The earth model adopted in the theoretical calculations is consisted of a two-layer crust of 38 km in thickness while the actual crustal thinkness of the propagation path over the Tibet plateau is likely to be greater than 50 km.

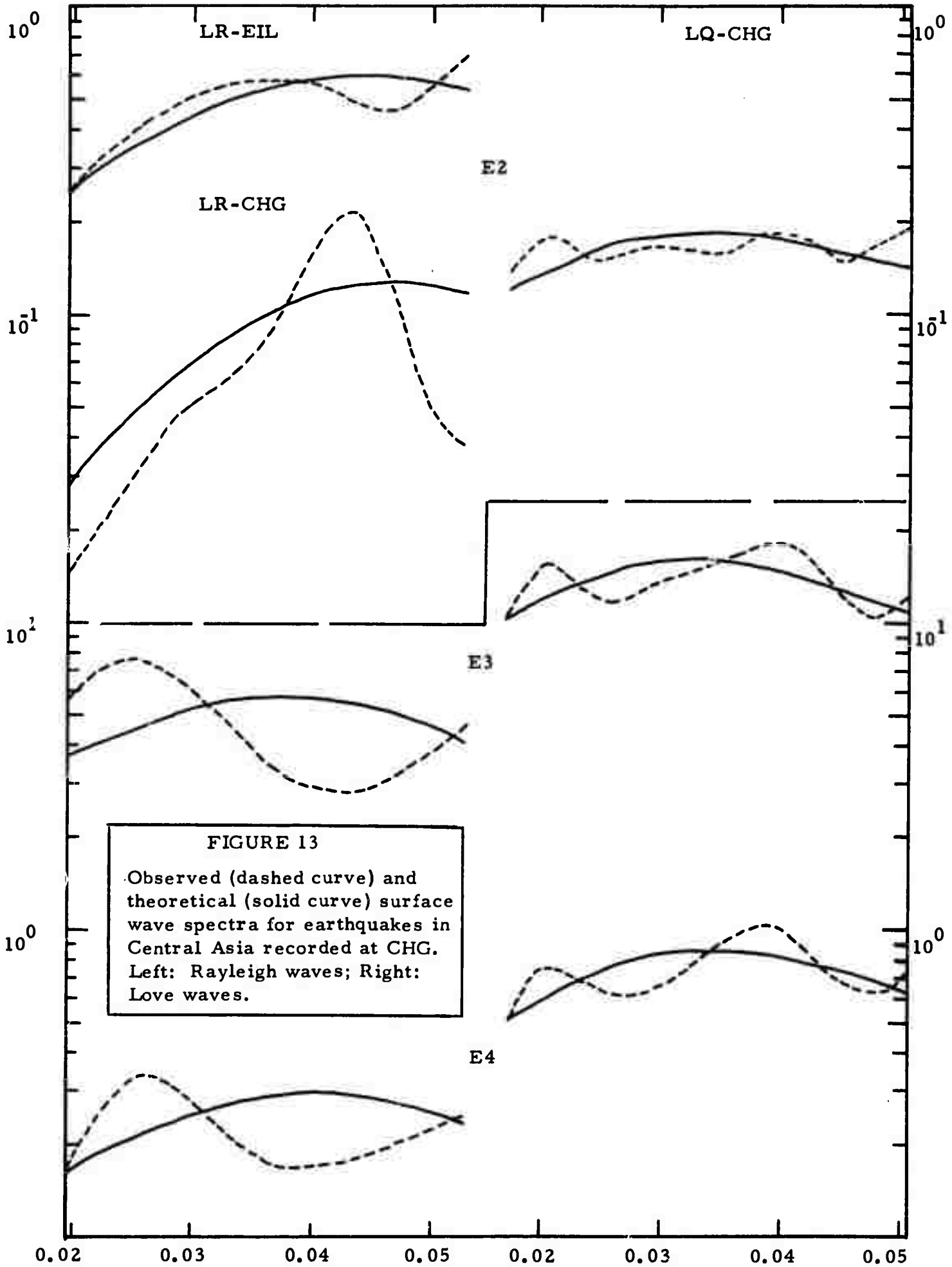

FIGURE 13

Observed (dashed curve) and theoretical (solid curve) surface wave spectra for earthquakes in Central Asia recorded at CHG. Left: Rayleigh waves; Right: Love waves.

(2) The observed Rayleigh wave spectrum is not adequately explained by the theoretical spectrum. This suggests that a flat-layered model is not enough to represent the actual earth structure from the epicenter to CHG.

To the best of our knowledge there is no fault-plane solution available for earthquakes in this region. We are in the process of obtaining some LP WWSSN P-wave data to make up this deficiency so that a more definitive interpretation can be made.

In summary, the results from the few test cases described above indicate that the automatic searching scheme based on a least-squares-error criterion can be applied to estimate some source parameters of earthquakes using surface wave spectral data at a few recording sites. The actual capability and limitations of such a scheme will be evaluated further when our data ensemble increases.

V. CONCLUSIONS AND FUTURE PLANS

Our work to date has resulted in the following conclusions:

(1) The complex cepstrum technique has proven to be a very effective means for removing the interference of surface waves due to multiple shocks or multipath propagation of a single shock or both. Application of the technique to actual surface wavetrains containing interfering events indicates that the technique may be capable of separating multiple events occurring as little as 20 seconds apart providing that the events are not multipathed as well. The technique has greatly enhanced the capability of the surface wave spectral analysis method to study seismic source characteristics.

(2) Because there are regional variations in the properties of both the seismic sources and the propagation media, we have started a study of surface wave spectra from seismic events in the Arctic Ocean and the Eurasian continent on a regional basis. The results of this study to date are:

(a) Rayleigh wave spectra from underground nuclear explosions in Novaya Zemlya appear to be similar from event to event and not to vary significantly with azimuth. Moreover, the difference in Rayleigh wave spectral shapes between these explosions and the earthquakes in the neighboring seismic zones is large enough to discriminate these explosions against a great majority of the earthquakes.

(b) For earthquakes in the Eurasian continent the shapes of both Rayleigh and Love wave spectra in the frequency range 0.02 to 0.05 Hz appear to vary very little among events taking place at the same location. This phenomemon may eventually enable us to set up a library of master spectra of surface waves. It is also found that Love wave spectra do not vary significantly among earthquakes even though they are located in different regions. On the contrary, Rayleigh wave spectra are highly variable among earthquakes from different locations. This phenomenon is consistent with theoretical predictions

made previously by Tsai and Aki (1970) and may be used to identify seismic sources of different regions.

(3) We have devised an automatic searching scheme on the basis of least-squares-error to find the best source model for a set of observed surface wave spectral data. The scheme has been tested on a very limited number of earthquakes in Eastern Turkey and Central Asia. The preliminary results are very promising.

In the coming months we intend to continue studying the surface wave spectral characteristics of seismic events in different regions. We shall make more intensive tests and refinements of the automatic searching scheme for source characterization by incorporating some body-wave data. It is hoped that the scheme eventually will enable us to make reliable estimates of some source parameters from the surface wave spectral data.

VI. REFERENCES

Canitez, N. and M. N. Toksoz, Focal mechanism and source depth of earthquakes from body- and surface-wave data, Bull. Seism. Soc. Am., 61, 1369-1379, 1971.

Linville, A. F., Rayleigh-wave multipath analysis using a complex cepstrum technique: Special Report No. 2, Texas Instruments, Incorporated, Service Group, Dallas, Texas, 1971.

Saito, M., Excitation of free oscillations and surface waves by a point source in a vertically heterogeneous earth, J. Geophys. Res., 72, 3689-3699, 1967.

Schafer, R. W., Echo removal by discrete generalized linear filtering: Technical Report 466, Mass. Inst. of Tech., Research Laboratory of Electronics, Cambridge, Mass., Ph. D. Thesis, 1969.

Skirokova, E. I., General features in the orientation of principal stresses in earthquake foci in the Mediterranean - Asian seismic belt, Izv. Earth Physics (English translation), No. 1, 22-36, 1967.

Sykes, L. R., Mechanism of earthquakes and nature of faulting on the mid-oceanic ridges, J. Geophys. Res., 72, 2131-2153, 1967.

Tsai, Y. B. and K. Aki, Precise focal depth determination from amplitude spectra of surface waves, J. Geophys. Res., 75, 5729-5743, 1970.

Tsai, Y. B. and K. Aki, Amplitude spectra of surface waves from small earthquakes and underground nuclear explosions, J. Geophys. Res., 76, 3940-3952, 1971.